Scientia Iranica, Vol. 10, No. 1, pp 91–102

SCIENTIA
IRANICA

Research Note

Upper Bound Analysis of Cylindrical Shells Subject to Local Bending Moments

G.H. Rahimi[1]

In this paper, a limit analysis of cylindrical shells with rectangular attachments well removed from the ends and subjected to local bending moments is performed. In the analysis, the upper bound technique is employed to give the minimum upper bound to the plastic limit load for a shell when it is subjected to local longitudinal and circumferential bending moments over a rectangular area of the cylindrical shell surface. In the analysis, a two-moment limited interaction yield surface is used. The results are presented for a range of practical geometrical parameters. An alternative collapse mechanism for longitudinal bending moment is examined.

INTRODUCTION

It is evident that certain areas of research concerning pressure vessel analysis have received a good deal more attention than others of no less importance from the viewpoint of design integrity and safety. One area which appears to have lacked intensive study is that of locally applied loads. Such loading conditions may arise at nozzles (where they may arise due to reactions of the piping system), lifting lugs, supports and other attachments causing local forces and moments. In practice, the analytical methods, based on the theory of elasticity, are most frequently used in solving this class of problems though many procedures are empirical.

Although many elastic formulations have been obtained, probably the most widely used are the shell solution provided by Bijlaard [1-4]. Wichman et al. [5] summarized this work by providing analytical design curves for cylindrical and spherical shells subjected to external loads. Also, more recent papers can be mentioned which deal with the elastic theoretical and experimental analysis of radial local loads [6,7]. But, for some special conditions of pressure vessels, for example, nuclear vessels, elasticity solutions are often inadequate. This is particularly true when considering the extremely large loads often defined for emergency and fault conditions. For most of these conditions, an elastic analysis greatly underestimates the load carrying capacity of the vessel. Therefore, for an adequate assessment, an analysis considering the plastic behavior of the structure must be performed.

The present work is concerned with the plastic behavior of cylindrical vessels when subjected to local bending moments. Here, the analytical bases are concerned with loads being applied over square or rectangular areas of a cylindrical shell. This is because the boundaries of such areas are easier to specify mathematically than, for example, that of a circular area, for which an analysis would be difficult. By employing a two-moment limited interaction yield surface, an upper bound has been found to the local limit load for a cylindrical shell with a rectangular attachment.

The introduction of a limit analysis as a computing tool has provided a powerful technique in many situations in engineering design. In the limit analysis, an elastic (or rigid), perfectly-plastic material model is assumed. The two well-known theorems of limit analysis, namely, the lower and upper bound theorems, are used to obtain an estimate of the limit load. The formal proofs of these theorems are well documented and can be found in many texts such as Symonds [8] and Hodge [9]. This paper is not concerned with the lower bound theorem which is based on equilibrium of external and internal forces. It uses the upper bound solution, since the effects of geometry for the present problem are such that a suitable kinematic pattern of plastic hinges can be associated with a limit load.

An upper bound analysis for the plastic limit moment of a cylindrical shell, subjected to a circumferential bending moment through a square attachment, was reported by Kitching et al. [10], along

1. *Department of Mechanical Engineering, Tarbiat Modares University, Tehran, I.R. Iran.*

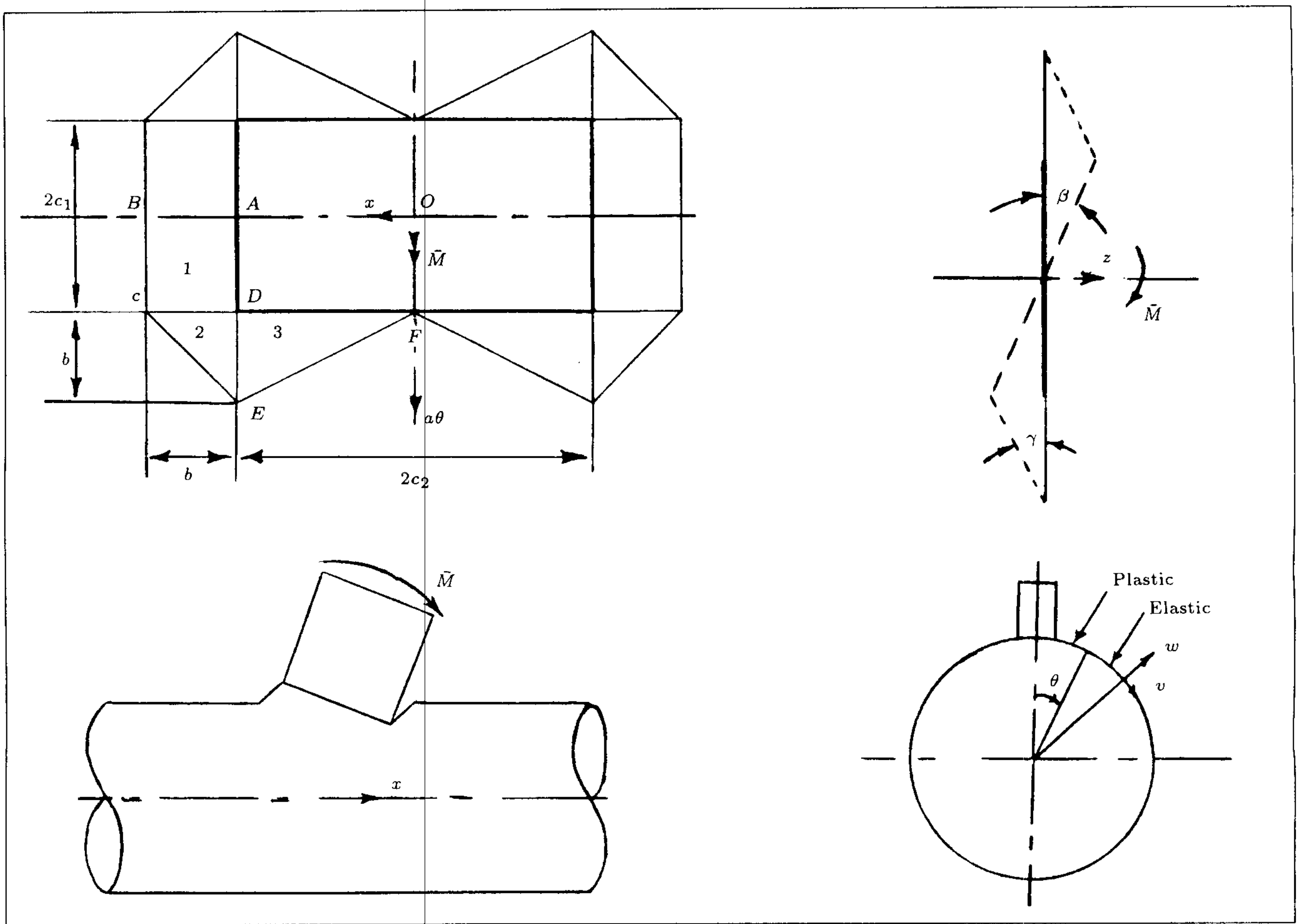

Figure 1. Longitudinal moment-notation and hinge pattern.

with the experimental behavior of 12 mild steel shells subjected to this type of loading. A similar analysis for cylindrical shells with square attachments subjected to longitudinal moments has been reported by Kitching et al. [11], along with experimental behavior of 14 specimens. Both analyses have used a two-moment limited interaction yield surface.

In this paper, these analyses [10,11] are extended for rectangular attachments with a modified collapse mechanism. A simple lower bound analysis for a cylindrical shell, when it is subjected to the local radial load through the rectangular attachments, is given in [12]. Also, an upper bound analysis of cylindrical shells subjected to local radial load has been presented by the author in [13].

UPPER BOUND CALCULATION FOR A CYLINDRICAL SHELL WITH A RECTANGULAR ATTACHMENT SUBJECTED TO LONGITUDINAL BENDING MOMENT

The presented analysis is similar to the analysis of [13] and is an extension of the work of [11] for rectangular attachments. It is also based on the assumptions of the analysis for radial loading of [13], for which the notation is the same where possible. Figure 1 shows the deformed shape of a surface of a shell around the attachment along with relevant hinge pattern. Because of symmetry about $\theta = 0$ and anti-symmetry about $x = 0$, it is necessary only to consider the internal energy dissipation of one quarter of the collapse mechanism, viz Regions 1, 2 and 3 of Figure 1, which are on the compression side of the attachment. For any point on the shell, the components of displacement in the x, θ and z directions are u, v and w, respectively. It is assumed that throughout the paper $u = 0$ and v, w, strains and curvatures are small. Curvatures and strains and twists at any point of the middle surface will be given by the following equations:

$$\varepsilon_x = u_{,x}, \quad \varepsilon_\theta = \frac{1}{a}(v_{,\theta} + w), \quad 2\varepsilon_{x\theta} = v_{,x}$$

$$k_x = -w_{,xx}, \quad k_\theta = \frac{1}{a^2}(v_{,\theta} - w_{,\theta\theta}),$$

$$2k_{x\theta} = \frac{1}{a}(v_{,x} - 2w_{,x\theta}). \qquad (1)$$

Using σ_0 as the yield stress in simple tension, defining N_0 and M_0 as $N_0 = \sigma_0 t$ and $M_0 = \frac{\sigma_0 t^2}{4}$, respectively (where t is the shell thickness), the two-moment limited yield surface is given by the following relations:

$$|N_\theta| = N_0, \quad |N_{x\theta}| = N_0/2,$$

$$|M_\theta| = M_0, \quad |M_{x\theta}| = M_0/2, \tag{2}$$

N_x and M_x are assumed zero within all regions (but not at the hinges).

The energy dissipation within any region is given by:

$$D_i = \iint N_0|\varepsilon_\theta| dx a d\theta + \iint 2\frac{N_0}{2}|\varepsilon_{x\theta}| dx a d\theta + \iint M_0|k_\theta| dx a d\theta + \iint 2\frac{M_0}{2}|k_{x\theta}| dx a d\theta, \tag{3}$$

where the limits of the integrals are appropriate for the regions.

The analysis for each of Regions 1, 2 and 3 is now given separately.

Region 1

It can be shown that $u = 0$ and $\gamma = \frac{\beta c_2}{b}$, hence:

$$w_1 = -\frac{\beta c_2}{b}(b + c_2 - x). \tag{4}$$

This gives $w_1 = 0$ at the hinge BC. Variable b indicates the extent of plastic deformation in the x direction. For circumferential movement in this region, inextensibility is assumed and this yields $\varepsilon_\theta = 0$, or $v_{,\theta} = w$, which gives:

$$v_1 = \frac{\beta c_2 \theta}{b}(b + c_2 - x). \tag{5}$$

Substituting Equations 4 and 5 into Equation 1 yields:

$$\varepsilon_x = k_x = \varepsilon_\theta = 0, \qquad \varepsilon_{x\theta} = -\frac{\beta c_2 \theta}{2b},$$

$$k_\theta = \frac{\beta c_2}{a^2 b}(b + c_2 - x), \quad k_{x\theta} = -\frac{\beta c_2 \theta}{2ab}.$$

Rotation at the hinge AD is $\beta+\gamma = \beta+\frac{\beta_2 c}{b}$ and rotation at the hinge BC is $\frac{\partial w}{\partial x} = \gamma = \frac{\beta c_2}{b}$. The total energy expended in Region 1 is:

$$\frac{D_1}{M_0 \beta c_2} = \frac{c_1}{c_2} + \frac{2c_2}{b} + \frac{N_0 c_1^2}{4M_0 a} + \frac{b c_1}{2a^2} + \frac{c_1^2}{4a^2}. \tag{6}$$

Region 2

Again, assume $u = 0$ and:

$$w_2 = -\frac{\beta c_2}{b}\big((b + c_2 - x) + (c_1 - a\theta)\big), \tag{7}$$

which gives continuity with Region 1 at $a\theta = c_1$ and $w_2 = 0$ along inclined hinge $a\theta = c_1 + c_2 + b - x$. It can also be shown that:

$$v_2 = \frac{\beta c_1 c_2}{ab}\big((b + c_2 - x) + (c_1 - a\theta)\big), \tag{8}$$

which gives continuity with Region 1 at $a\theta = c_1$ and also gives $v_2 = 0$ along inclined hinge EC. Strains and curvatures are:

$$\varepsilon_x = k_x = 0, \quad \varepsilon_\theta = -\frac{\beta c_2}{ab}(b + 2c_1 + c_2 - a\theta),$$

for which the bracket is always positive and ε_θ negative and:

$$\varepsilon_{x\theta} = -\frac{\beta c_1 c_2}{2ab}, \quad k_\theta = -\frac{\beta c_1 c_2}{a^2 b}, \quad k_{x\theta} = -\frac{\beta c_1 c_2}{2a^2 b}.$$

Rotation at boundary with Region 1 is $\frac{\partial w}{a\partial\theta} = \frac{\beta c_2}{b}$ and rotation at boundary with Region 3 is $\frac{\partial w}{\partial x} = \frac{\beta c_2}{b}$.

Rotation at inclined boundary is $|\frac{w_{,\theta}}{a\sqrt{2}} + \frac{w_{,x}}{\sqrt{2}}| = \frac{2\beta c_2}{\sqrt{2}b}$.

Total energy dissipation in Region 2 will be:

$$\frac{D_2}{M_0 \beta c_2} = 4 + \frac{3bc_1}{4a^2} + \frac{3N_0 b c_1}{4M_0 a} + \frac{N_0 b^2}{6M_0 a}. \tag{9}$$

Region 3

Again $u = 0$ and:

$$w_3 = -\frac{\beta c_2}{b}\Big(\frac{bx_2}{c_2} + c_1 - a\theta\Big), \tag{10}$$

which gives $w_3 = -\beta c_2$ at ($x = c_2$ and $a\theta = c_1$) as required, and $w_3 = 0$ at ($x = 0, c_2$ and $a\theta = c_1, b + c_1$) and $w_3 = 0$ at the inclined hinge. Furthermore, one can construct:

$$v_3 = \frac{\beta c_1 c_2}{ab}\Big(c + \frac{bx}{c_2} - a\theta\Big). \tag{11}$$

Thus:

$$\varepsilon_x = k_x = 0, \quad \varepsilon_\theta = \frac{-\beta c_2}{ab}\Big(2c_1 + \frac{bx}{c_2} - a\theta\Big),$$

$$\varepsilon_{x\theta} = \frac{\beta c_1}{2a}, \quad k_\theta = \frac{-\beta c_1 c_2}{a^2 b}, \quad k_{x\theta} = \frac{\beta c_1}{2a^2}.$$

Rotation at boundary with attachment is $\frac{\partial w}{a\partial\theta} = \frac{\beta c_2}{b}$, and rotation at boundary with Region 2 is $\frac{\partial w}{\partial x} = \beta$.

Rotation at inclined hinge is:

$$\left(b\frac{\partial w}{\partial x} - c_2\frac{\partial w}{a\partial\theta}\right)\frac{1}{\sqrt{b^2+c_2^2}} = \frac{\beta\sqrt{b^2+c_2^2}}{b}.$$

Therefore, total energy dissipation in Region 3 will be:

$$\frac{D_3}{M_0\beta c_2} = \frac{2b}{c_2} + \frac{2c_2}{b} + \frac{N_0c_1c_2}{2M_0a} + \frac{N_0c_2b}{6M_0a} + \frac{N_0bc_1}{4M_0a} + \frac{c_1c_2}{2a^2} + \frac{bc_1}{4a^2}. \tag{12}$$

Energy Balance

Now, equating external work done to total internal energy dissipation for the complete mechanism gives $\bar{M}_l\beta = 4(D_1 + D_2 + D_3)$ where $\bar{M}_l$ is the bending moment applied to the attachment. Writing the non-dimensional moment as:

$$M_l^* = \frac{\bar{M}_l}{4M_0c_2} = \frac{c_1}{c_2} + \frac{2c_2}{b} + \frac{2c_1}{b} + \frac{c_1^3}{at} + \frac{3bc_1}{4a^2} + \frac{c_1^2}{4a^2} + 4 + \frac{4bc_1}{at} + \frac{2b^2}{3at} + \frac{2b}{c_2} + \frac{2c_1c_2}{at} + \frac{2bc_2}{3at} + \frac{c_1c_2}{2a^2}, \tag{13}$$

and using the non-dimensional geometric parameters:

$$\Omega = \frac{b}{c_1}, \quad \gamma = \frac{c_1}{a}, \quad \rho^2 = \frac{c_1^2}{at}, \quad \alpha = \frac{c_1}{c_2},$$

Equation 13 can be, therefore, rewritten as :

$$M_l^* = \left(4 + \alpha + \frac{2}{\Omega} + \frac{3}{\alpha\Omega} + 2\alpha\Omega\right) + \rho^2\left(1 + 4\Omega + \frac{2\Omega^2}{3} + \frac{2}{\alpha} + \frac{2\Omega}{3\alpha}\right) + \gamma^2\left(\frac{3\Omega}{2} + \frac{1}{2\alpha} + \frac{1}{4}\right). \tag{14}$$

Parameters α, γ and ρ are given, so that the minimum value of M_l^* is given by $\frac{M_l^*}{\partial\Omega} = 0$, or:

$$\frac{4}{3}\rho^2\Omega^3 + \left(2a + \frac{3\gamma^2}{2} + 4\rho^2 + \frac{2\rho^2}{3a}\right)\Omega^2 - 2\left(1 + \frac{1}{\alpha}\right) = 0. \tag{15}$$

Solution of Equation 15 for various values of α, γ and ρ gives Ω which, in turn, gives a minimum value of M_l^*. Figures 2a and 2b show the curves of M_l^* against ρ for various values of α and γ.

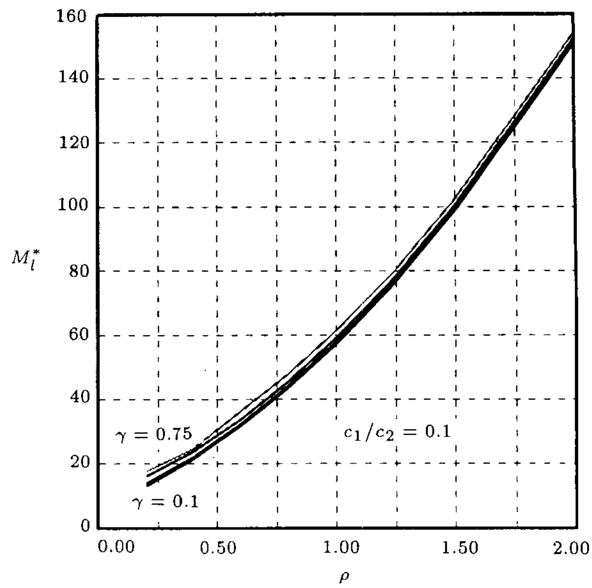

Figure 2a. Limit axial moment versus ρ for $\alpha = 0.1$.

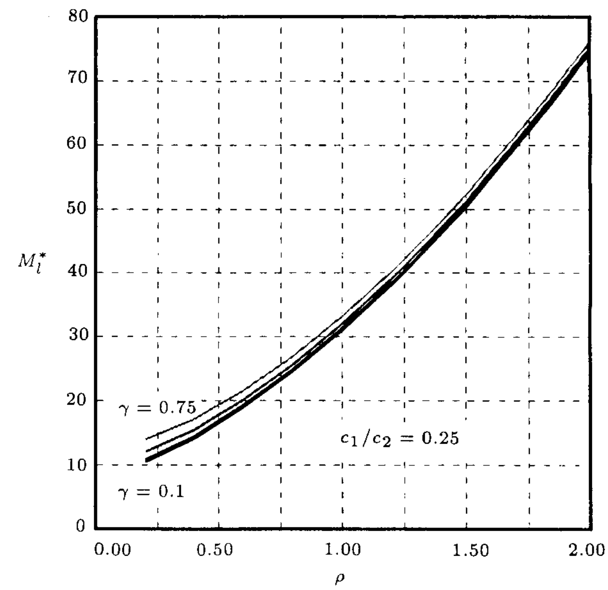

Figure 2b. Limit axial moment versus ρ for $\alpha = 0.25$.

ALTERNATIVE COLLAPSE MECHANISM-LONGITUDINAL BENDING MOMENT

An improvement on the results of [11] for an upper bound for a square attachment is expected if the extent of the plastic zone in the axial direction (b) is different from that in the circumferential direction (d). In the analysis of [11], b and d were equal. An analysis with b and d as different parameters is now given. Figure 3 shows the hinge pattern along with the appropriate dimension and notation. The kinematic relations of Equation 1 are used and plastic limit moment $\bar{M}_l$ is calculated by considering the shell to be divided

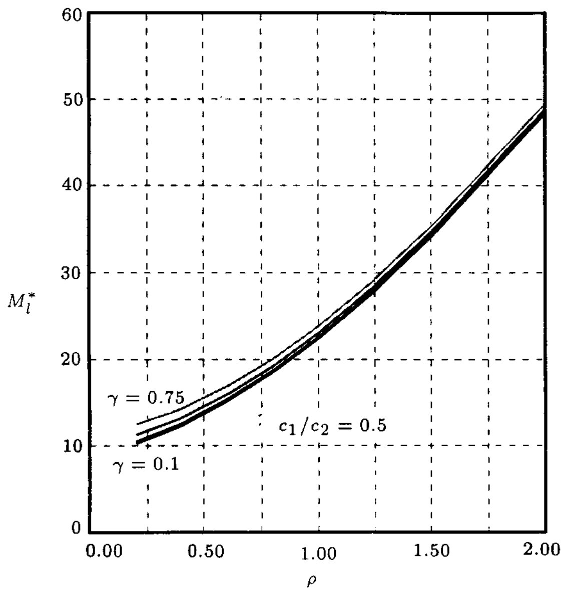

Figure 2c. Limit axial moment versus ρ for $\alpha = 0.5$.

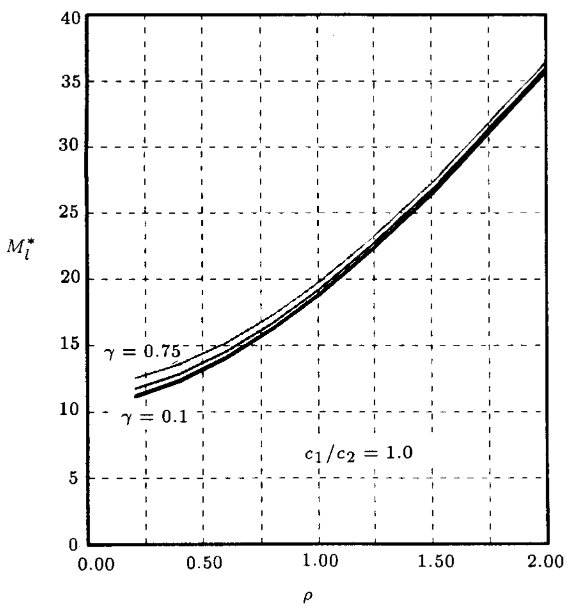

Figure 2d. Limit axial moment versus ρ for $\alpha = 1.0$.

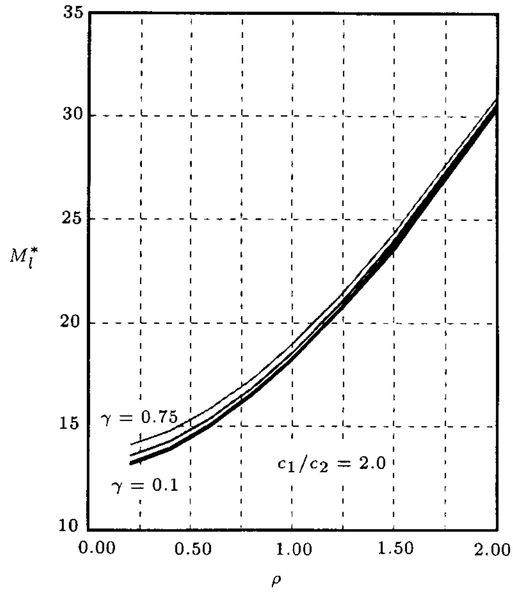

Figure 2e. Limit axial moment versus ρ for $\alpha = 2.0$.

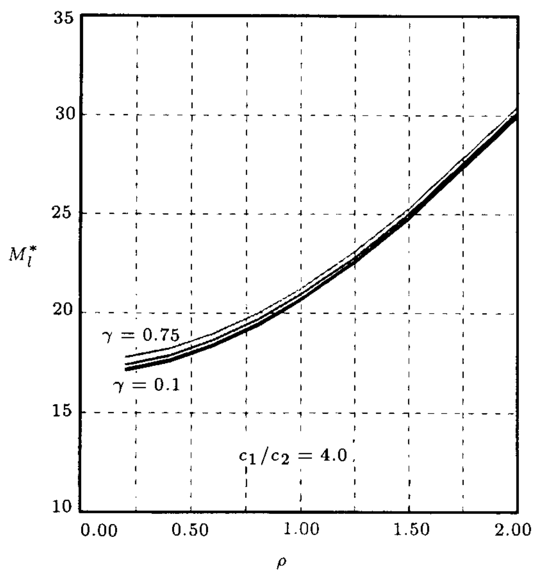

Figure 2f. Limit axial moment versus ρ for $\alpha = 4.0$.

into regions, the collapse mechanism being shown in Figure 3.

Region 1

$$u = 0, \quad w_1 = -\frac{\beta c}{b}(b + c - x), \tag{16}$$

$$v_1 = \frac{\beta c\theta}{b}(b + c - x), \tag{17}$$

strains and curvatures are:

$$\varepsilon_x = k_x = \varepsilon_\theta = 0, \quad \varepsilon_{x\theta} = -\frac{\beta c\theta}{2b},$$

$$k_{x\theta} = -\frac{\beta c\theta}{2ab}, \qquad k_\theta = \frac{\beta c}{a^2 b}(b + c - x).$$

Rotation at the hinge AD is $\beta + \alpha = \beta + \frac{\beta c}{b}$ and at the hinge BC is $\frac{\partial w}{\partial x} = \gamma = \frac{\beta c}{b}$.

The total energy dissipation in Region 1 is given by:

$$\frac{D_1}{M_0\beta c} = \frac{N_0 c^2}{4M_0 a} + \frac{c^2}{4a} + \frac{bc}{2a^2} + 1 + \frac{2c}{b}. \tag{18}$$

Region 2

To be compatible with Region 1 at the common boundary the following is written:

$$w_2 = -\beta c\Big(\frac{b + c - x}{b} + \frac{c - a\theta}{d}\Big), \tag{19}$$

$$v_2 = \frac{\beta c^2}{a}\Big(\frac{b + c - x}{b} + \frac{c - a\theta}{d}\Big). \tag{20}$$

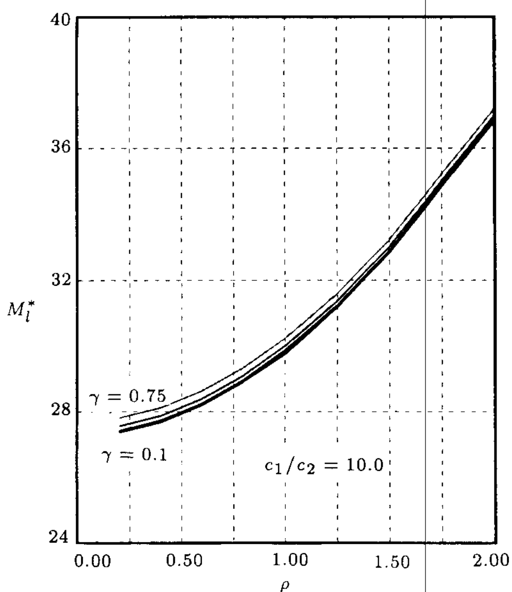

Figure 2g. Limit axial moment versus ρ for $\alpha = 10.0$.

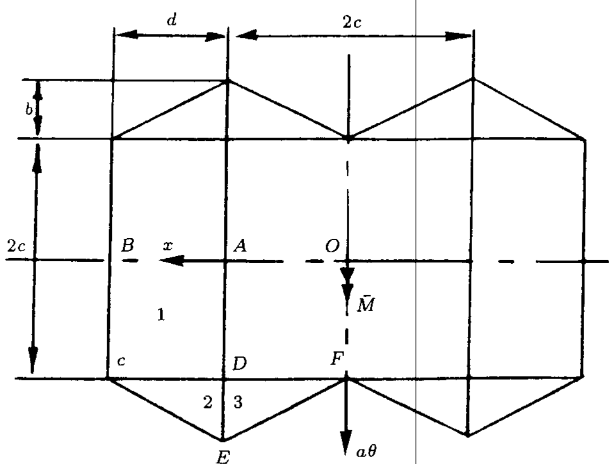

Figure 3. Alternative hinge pattern.

Substituting w_2 and v_2 into Equation 1 gives:

$$\varepsilon_x = k_x = 0, \quad \varepsilon_\theta = -\frac{\beta c}{abd}(2bc+bd+cd-xd-ab\theta),$$

$$\varepsilon_{x\theta} = -\frac{\beta c^2}{2ab}, \quad k_\theta = -\frac{\beta c^2}{a^2 d}, \quad k_{x\theta} = \frac{-\beta c^2}{2a^2 b}.$$

Rotation at boundary with Region 1 is $\frac{\partial w}{a\partial\theta} = \frac{\beta c}{d}$ and rotation at boundary with Region 3 is $\frac{\partial w}{\partial x} = \frac{\beta c}{b}$.

Rotation at inclined boundary is $\left(b\frac{\partial w}{\partial x} + d\frac{\partial w}{a\partial\theta}\right)\frac{1}{\sqrt{b^2+d^2}} = \frac{2\beta c}{\sqrt{b^2+d^2}}$.

Total energy dissipation in Region 2 will be:

$$\frac{D_2}{M_0\beta c} = 2 + \frac{b}{d} + \frac{d}{b} + \frac{N_0 cd}{4M_0 ab}(2b-d) + \frac{3c}{4a^2}(2b-d)$$
$$+ \frac{N_0}{M_0 ab}\left(b^2 c + \frac{bd^2}{3} - \frac{bdc}{2} - \frac{d^3}{6}\right). \tag{21}$$

Region 3

To be compatible with Region 2 at a common boundary and to ensure that the moment of a point at the edge of the attachment is parallel to the longitudinal centre line of the attachment, one has $u = 0$ and:

$$w_3 = -\frac{\beta c}{d}\left(c + \frac{dx}{c} - a\theta\right), \tag{22}$$

$$v_3 = -\frac{\beta c^2}{ad}\left(c + \frac{dx}{c} - a\theta\right). \tag{23}$$

Therefore,

$$\varepsilon_x = k_x = 0, \quad \varepsilon_\theta = -\frac{\beta c}{ad}\left(2c + \frac{dx}{c} - a\theta\right),$$

$$\varepsilon_{x\theta} = \frac{\beta c}{2a}, \quad k_\theta = -\frac{\beta c^2}{a^2 d}, \quad k_{x\theta} = \frac{\beta c^2}{2a^2}.$$

Rotation at the boundary with attachment is $\frac{\partial w}{a\partial\theta} = \frac{\beta c}{d}$, rotation at the boundary with Region 2 is $\frac{\partial w}{\partial x} = \beta$ and rotation at the inclined hinge is $\frac{\beta\sqrt{d^2+c^2}}{d}$.

Hence, the total energy dissipation in Region 3 is:

$$\frac{D_3}{M_0\beta c} = \frac{2c}{d} + \frac{2d}{c} + \frac{N_0 c}{2M_0 a}\left(c + \frac{d}{3}\right)$$
$$+ \frac{N_0 cd}{4M_0 a} + \frac{c^2}{4a^2} + \frac{dc}{4a^2}. \tag{24}$$

Energy Balance

The expressions in Equations 18, 21 and 24 may now be used to equate the external work done and the total energy dissipated in the four quadrants of the cylinder to get:

$$M_l^* = \frac{\bar{M}}{4M_0 c} = 3 + \frac{2c}{b} + \frac{d}{b} + \frac{b}{d} + \frac{2c}{d} + \frac{2d}{c} + \frac{3c^2}{at} + \frac{3c^2}{4a^2}$$
$$+ \frac{2bc}{a^2} + \frac{4bc}{at} + \frac{5dc}{3at} - \frac{cd}{2a^2} + \frac{4d^2}{3at} - \frac{2d^2}{3abt} - \frac{cd^2}{atb}, \tag{25}$$

where $\bar{M}$ and M_l^* are plastic limit moment and non-dimensional limit moment, respectively. If it is assumed that $\Omega_1 = \frac{b}{c}$, $\Omega_2 = \frac{d}{c}$, $\gamma = \frac{c}{a}$ and $\rho^2 = \frac{c^2}{at}$, Equation 25 becomes:

$$M_l^* = \left(3 + \frac{2}{\Omega_1} + \frac{\Omega_1}{\Omega_2} + \frac{\Omega_2}{\Omega_1} + \frac{2}{\Omega_2} + 2\Omega_2\right)$$
$$+ \rho^2\left(3 + 4\Omega_1 + \frac{5\Omega_2}{3} + \frac{4\Omega_2^2}{3} - \frac{2\Omega_2^3}{3\Omega_1} - \frac{\Omega_2^2}{\Omega_1}\right)$$
$$+ \gamma^2\left(\frac{3}{4} + 2\Omega_1 - \frac{\Omega_2}{2}\right). \tag{26}$$

Since $M_l^*(\Omega_1, \Omega_2)$ can never be less than zero, it is known that its minimum value is finite and must occur

Table 1. Comparison of two collapse mechaisms results.

ρ	Results of Assumed Mechanism in the Second Section ($\alpha = 1$)			Results of the First Section and [11] ($\alpha = 1$)	
	Ω_1	Ω_2	M_l^*	Ω	M_l^*
0.0	2.042	1.274	10.324	1.414	11.00
0.2	1.759	1.192	10.85	1.337	11.08
0.4	1.319	1.061	12.185	1.158	12.30
0.6	0.988	0.974	13.998	0.985	13.00
0.8	0.725	1.055	16.084	0.837	16.17
1.0	0.568	1.016	18.163	0.724	18.70
1.2	0.534	0.675	21.222	0.639	22.046
1.4	0.527	0.335	26.52	0.563	25.00
1.6	0.446	0.409	28.534	0.509	28.07
1.8	0.217	0.384	32.998	0.458	31.747
2.0	0.346	0.086	54.343	0.418	35.70

at a point (for each certain value of ρ and γ), where the first partial derivatives vanish:

$$\frac{\partial M^*}{\partial \Omega_1} = -\frac{2}{\Omega_1^2} + \frac{1}{\Omega_2} - \frac{\Omega_2}{\Omega_1^2} + \rho^2\Big(4 + \frac{2\Omega_2^3}{3\Omega_1^2} + \frac{\Omega_2^2}{\Omega_1^2}\Big) + 2\gamma^2 = 0,$$

$$\frac{\partial M^*}{\partial \Omega_2} = -\frac{\Omega_1}{\Omega_2^2} + \frac{1}{\Omega_1} - \frac{2}{\Omega_2^2} + 2 + \rho^2\Big(\frac{5}{3} + \frac{8}{3}\Omega_2 - \frac{2\Omega_2^2}{\Omega_1} - \frac{2\Omega_2}{\Omega_1}\Big) - \frac{\gamma^2}{2} = 0. \tag{27}$$

The solving of this system of non-linear equations gives Ω_1 and Ω_2 for the minimum value of M_l^*. The Newton-Raphson method is employed to solve the above equations and to obtain the corresponding minimum M_l^* for certain values of parameters $a(=1)$, $\gamma(=0.0)$ and $\rho(=0.0$ to $2.0)$. Table 1 shows the results, along with the corresponding values of M_l^* and Ω taken from [11].

UPPER BOUND CALCULATION FOR A CYLINDRICAL SHELL WITH A RECTANGULAR ATTACHMENT SUBJECTED TO HOOP BENDING MOMENT

The analysis is similar to the analysis for a cylindrical shell with a square attachment [10]. The assumptions of the first section and kinematic relations are again employed. Figure 4 shows the notations, sign convention, displacement and the deformed shape of the shell surface around the attachment, together with a corresponding hinge pattern. Here, with reference to the analysis of the second section, b and d are made equal.

Region 1

Since $u = 0$:

$$w_1 = \frac{-\beta c_2}{b}(b + c_1 - a\theta), \tag{28}$$

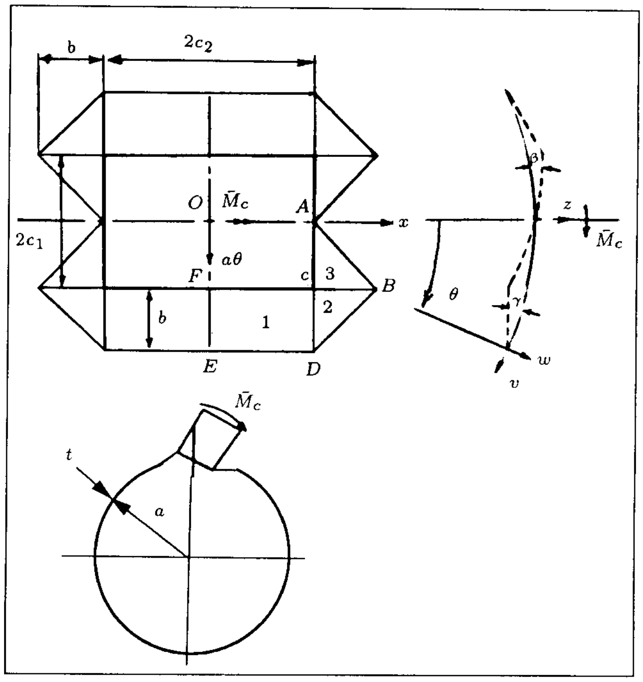

Figure 4. Hoop moment-notation and sign conventions.

where β is angular rotation of the rectangular pad. Assuming ε_θ is constant for the Region 1 and making $v_1 = 0$ at the hinges FC and ED, hence, the following is obtained:

$$v_1 = \frac{\beta c_2}{b}\left(\Big(b + c_1\Big)\Big(\theta - \frac{c_1}{2a}\Big) - \frac{b\theta}{2} - \frac{a\theta^2}{2}\right), \tag{29}$$

and strains and curvatures are:

$$\varepsilon_\theta = \varepsilon_{x\theta} = k_x = k_{x\theta} = 0,$$

$$\varepsilon_\theta = -\frac{\beta c_2}{2a}, \quad k_\theta = \frac{\beta c_2}{a^2 b}\Big(\frac{b}{2} + c_1 - a\theta\Big).$$

Rotation at the hinge FC is $\beta + \gamma = \beta + \frac{\beta c_2}{b}$ and rotation at the hinge ED is $\gamma = \frac{\beta c_2}{b}$.

The total energy dissipated in Region 1 will be:

$$D_1 = M_0 c_2\Big(\beta + \frac{\beta c_2}{b}\Big) + M_0 c_2 \frac{\beta c_2}{b} + \int_{x=0}^{c_2}\int_{\theta=c_1/a}^{(b+c_2)/b} N_0 \Big| -\frac{\beta c_2}{2a}\Big| a\, d\theta\, dx + \cdots,$$

$$\frac{D_1}{M_0 \beta c_2} = 1 + \frac{2c_2}{b} + \frac{bc_2}{4a^2} + \frac{N_0 c_1 c_2}{2M_0 a}. \tag{30}$$

Region 2

To be compatible with Region 1 and zero at the inclined hinge $a\theta = c_1 + c_2 + b - x$:

$$w_2 = -\frac{\beta c_2}{b}(b + c_1 + c_2 - x - a\theta), \tag{31}$$

v_2 can be constructed from the requirements that $v_2 = 0$ along the inclined hinge and $v_2 = v_1$ at $x = c_2$, therefore;

$$v_2 = -\frac{\beta c_2}{2ab}(b + c_2 + c_1 - x - a\theta)^2 + \frac{\beta c_2}{2ab}(b + c_2 - x)(b + c_1 + c_2 - x - a\theta). \quad (32)$$

Strains and curvatures are:

$$\varepsilon_x = k_x = 0,$$

$$\varepsilon_\theta = -\frac{\beta c_2}{2ab}(b + c_2 - x),$$

$$\varepsilon_{x\theta} = \frac{\beta c_2}{4ab}(c_1 - a\theta),$$

$$k_\theta = \frac{\beta c_2}{2a^2 b}(b + 2c_1 + c_2 - x - a\theta),$$

$$k_{x\theta} = \frac{\beta c_2}{4a^2 b}(c_1 - a\theta).$$

Rotation at the boundary with Region 1 is $\frac{\partial w_2}{\partial x} = \frac{\beta c_2}{b}$, and rotation at the boundary with Region 3 is $\frac{\partial w_2}{a\partial\theta} = \frac{c_2}{b}$.

Energy dissipation in Region 2 will be:

$$D_2 = 4M_0\beta c_2 + \int_{\theta=c_1/a}^{(b+c_1)/a} \int_{x=c_2}^{b+c_1+c_2-a\theta} N_0|\varepsilon_\theta|dx\,ad\theta + \cdots,$$

$$\frac{D_2}{M_0\beta c_2} = 4 + \frac{5N_0 b^2}{24M_0 a} + \frac{b^2}{8a^2}. \quad (33)$$

Region 3

To be compatible with Region 2 at a common boundary with the rigid attachment and to give $w_3 = 0$ at the inclined hinge $a\theta = \frac{c_1}{b}(x - c_2)$ requires:

$$w_3 = -\frac{\beta c_2}{b}\Big(\frac{ab\theta}{c_1} - x + c_2\Big). \quad (34)$$

A suitable expression for v_3, giving $v_3 = 0$ at the boundary with attachment, at the inclined hinge and at the junction with Region 2, is:

$$v_3 = \frac{\beta c_2^2}{2ab^2}\Big(\frac{ab\theta}{c_1} - x + c_2\Big)^2 - \frac{\beta c_2^2\theta}{2b^2 c_1}\Big(\frac{ab\theta}{c_1} - x + c_2\Big)\Big(b - x + c_2\Big). \quad (35)$$

Strains and curvatures are :

$$\varepsilon_\theta = \frac{\beta c_2^2}{2ab}\left(2\Big(\frac{ab\theta}{c_1} - x + c_2\Big)\Big(\frac{1}{c_1} - \frac{1}{c_2}\Big) - \frac{1}{c_1}\Big(b - x + c_2\Big)\Big(\frac{2a\theta}{c_1} + \frac{c_2 - x}{b}\Big)\right),$$

$$\varepsilon_{x\theta} = \frac{-\beta c_2^2}{4ab^2}\Big(\frac{ab\theta}{c_1} + 2c_2 - 2x\Big)\Big(1 - \frac{a\theta}{c_1}\Big),$$

$$k_\theta = \frac{\beta c_2^2(c_2 - x)}{2a^2 bc_1}\Big(1 + \frac{x - c_2}{b} - \frac{2a\theta}{c_1}\Big),$$

$$k_x = -\frac{\beta c_2^2}{4a^2 b^2}\Big(\frac{ab\theta}{c_1} + 2c_2 - 2x\Big)\Big(1 - \frac{a\theta}{c_1}\Big).$$

Rotation at the boundary with attachment is $\frac{\partial w_3}{\partial x} = \frac{\beta c_2}{b}$, rotation at the boundary with Region 2 is $\frac{\partial w_3}{ad\theta} = \frac{\beta c_2}{c_1}$, and rotation at the inclined hinge AB is $\frac{\beta c_2}{bc_1}\sqrt{b^2 + c_1^2}$.

The total energy dissipation in Region 3 will be:

$$\begin{aligned} D_3 =& M_0 c_1 + \frac{\beta c_2}{b} + M_0 b\frac{\beta c_2}{c_1} + \frac{M_0\beta c_2}{bc_1}(b^2 + c_1^2) \\ &+ \int_{x=c_2}^{b+c_2} \int_{\theta=c_1(x-c_2)/ab}^{c_1/a} N_0|\varepsilon_\theta|d\theta\,adx \\ &+ \int_{\theta=0}^{c_1/a} \int_{x=c_2}^{c_2+\frac{ab\theta}{2c_1}} N_0|\varepsilon_{x\theta}|dx\,ad\theta \\ &+ \int_{\theta=0}^{c_1/a} \int_{x=c_2+\frac{ab\theta}{2c_1}}^{c_2+\frac{ab\theta}{2c_1}} -N_0|\varepsilon_{x\theta}|d\theta\,adx \\ &+ \int_{x=c_2}^{b+c_2} \int_{\theta=c_1(x-c_2)/ab}^{c_1(b+x-c_2)/2ab} M_0|k_\theta|d\theta\,adx + \cdots, \end{aligned}$$

$$\frac{D_3}{M_0\beta c_2} = \frac{2c_1}{b} + \frac{2b}{c_1} + \frac{bc_2}{48a^2} + \frac{c_1 c_2}{24a^2} + \frac{N_0 c_1 c_2}{24M_0 a} + \frac{N_0 bc_1}{6M_0 a}. \quad (36)$$

The total energy dissipated in the four quadrants of the cylinder may now be equated with external work done and gives:

$$M_c^* = \frac{\bar{M}}{4M_0 c_2} = 5 + \frac{2c_2}{b} + \frac{2c_1}{b} + \frac{2b}{c_1} + \frac{13c_1 c_2}{6at} + \frac{5b^2}{6at} + \frac{b^2}{8a^2} + \frac{13bc_2}{48a^2} + \frac{c_1 c_2}{24a^2} + \frac{2bc_1}{3at}. \quad (37)$$

Using the non-dimensional geometric parameters:

$$\Omega = \frac{b}{c_1}, \quad \alpha = \frac{c_1}{c_2}, \quad \gamma = \frac{c_1}{a}, \quad \rho^2 = \frac{c_1^2}{at},$$

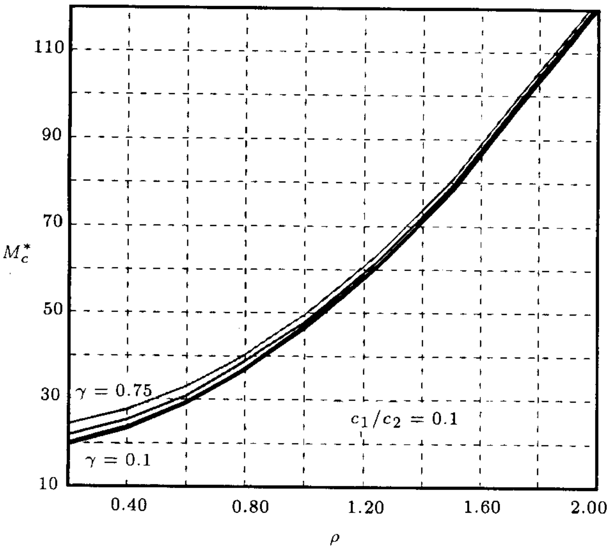

Figure 5a. Limit hoop moment versus ρ for $\alpha = 0.1$.

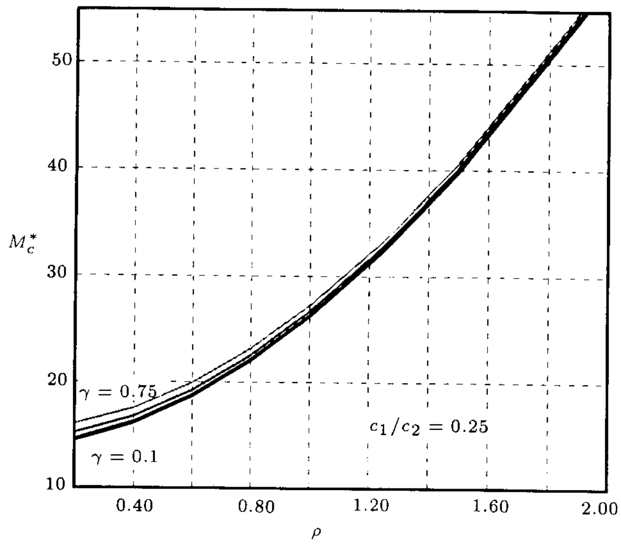

Figure 5b. Limit hoop moment versus ρ for $\alpha = 0.25$.

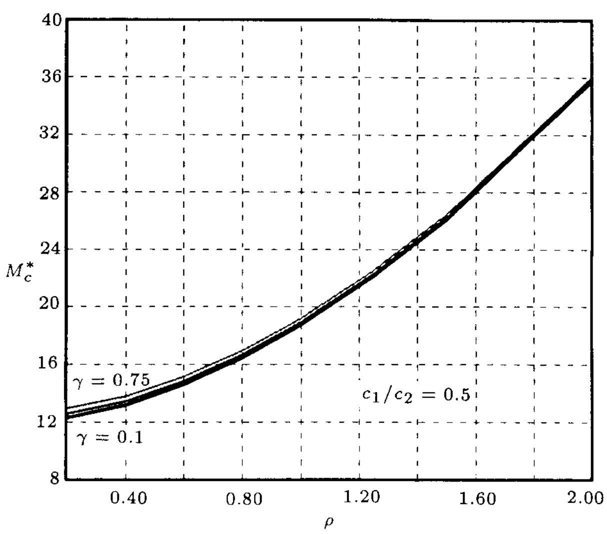

Figure 5c. Limit hoop moment versus ρ for $\alpha = 0.5$.

it is obtained that:

$$M_c^* = \left(5 + \frac{2}{\alpha\Omega} + \frac{2}{\Omega} + 2\Omega\right) + \rho^2\left(\frac{13}{6\alpha} + \frac{5\Omega^2}{6} + \frac{2\Omega}{3}\right) + \gamma^2\left(\frac{\Omega^2}{8} + \frac{13\Omega}{48a} + \frac{1}{24a}\right). \tag{38}$$

The parameter Ω is a variable and may be adjusted to give a minimum for M_c^* by solving the cubic equation $\frac{\partial M_c^*}{\partial \Omega} = 0$, or:

$$\alpha\left(\frac{5\rho^2}{3} + \frac{\gamma^2}{4}\right)\Omega^3 + \left(\frac{2\rho^2\alpha}{3} + \frac{13\gamma^2}{48} + 2\alpha\right)\Omega^2 - 2(1+\alpha) = 0. \tag{39}$$

The solution of Equation 39 for various values of α, γ and ρ gives Ω, which, substituting in Equation 38, gives a minimum value of M_c^*. Figures 5 illustrates the curves of M_c^* against ρ for various values of γ and α.

DISCUSSION OF RESULTS

In Figures 2 and 5 the upper bound to the non-dimensional limit longitudinal moment and circumferential moment for an open ended cylindrical shell are plotted, respectively, against the parameter $\rho(= \frac{c_1}{\sqrt{at}})$ for various values of $\gamma(= \frac{c_1}{a})$ and $\alpha(= \frac{c_1}{c_2})$. The results have been computed using Equations 14 and 38. It has been assumed that the cylindrical shell is long enough for the influence of the ends to be neglected. The theoretical work indicates that when the shell is subjected to a local load, only, as a consequence, a small local region becomes plastic. The position $\theta = \frac{b+c_1}{a}$ in the circumferential direction (and also $x = b + c_2$ in the axial direction) of the boundary, separating the plastic from the rigid region, is one of the unknowns of the problem.

The most significant results of the analysis are outlined as follows:

1. A comparison of Figures 2 and 5 shows that the two sets of curves illustrate, approximately, the same behavior. This may be because the same analysis procedure is employed throughout using similar hinge patterns for all cases of loading. These figures suggest that there is a continuous and consistent relationship between applied loads and ρ. The figures also indicate that, as the parameter ρ becomes bigger, the corresponding limit load gets bigger in value;

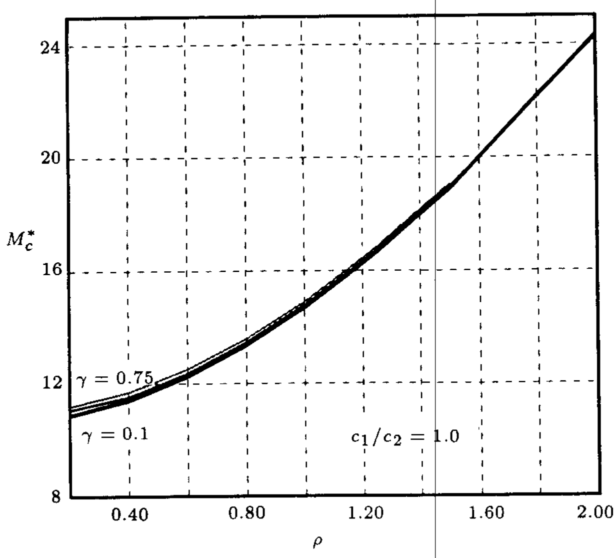

Figure 5d. Limit hoop moment versus ρ for $\alpha = 1.0$.

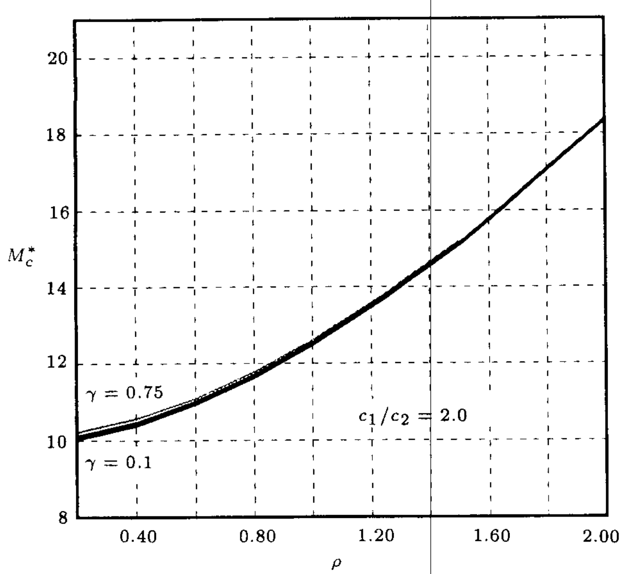

Figure 5e. Limit hoop moment versus ρ for $\alpha = 2.0$.

2. For many practical situations, γ^2 is small enough to make the third term in the above mentioned equations negligible. The resulting values of M_l^* and M_c^* will still become upper bound to the (non-dimensional) limit load, but will be close to the limit load. Of course, it appears that corresponding to neglecting energy dissipation due to loading within the plastic zones, gives results only marginally different from those with $\gamma \neq 0$. Neglecting of γ for the simplification of calculations is in the order of ignoring the bending strain energy within the regions.

   Comparison between [10] (p 79, Table 3) and Figures 5 of the present work shows that, as ρ increases, the discrepancy between the results becomes more significant (e.g., maximum 16% for $\rho = 2$) but for small values of ρ ($\rho < 1$) they are approximately coincident. Results of the theoretical analysis show little influence by γ, so the assumption is justified. Figures 2 and 5 show that for each fixed value of α, the change of γ has little effect on the limit load, though as γ rises the limit load increases a little. The influence of γ decreases as ρ increases and sometimes the curves are coincident for the range of γ investigated;

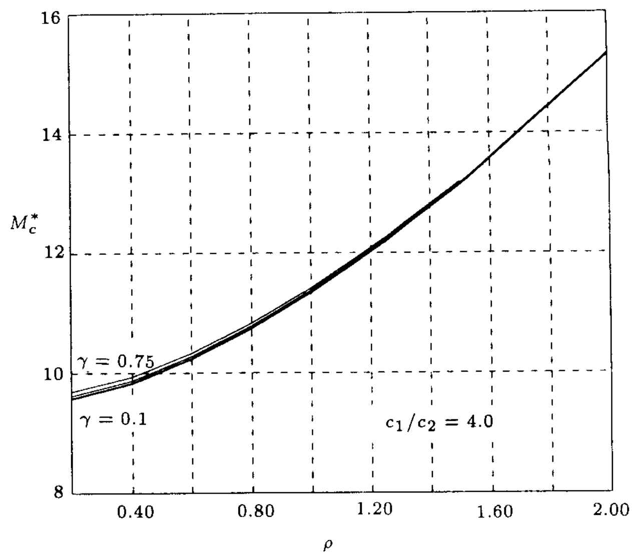

Figure 5f. Limit hoop moment versus ρ for $\alpha = 4.0$.

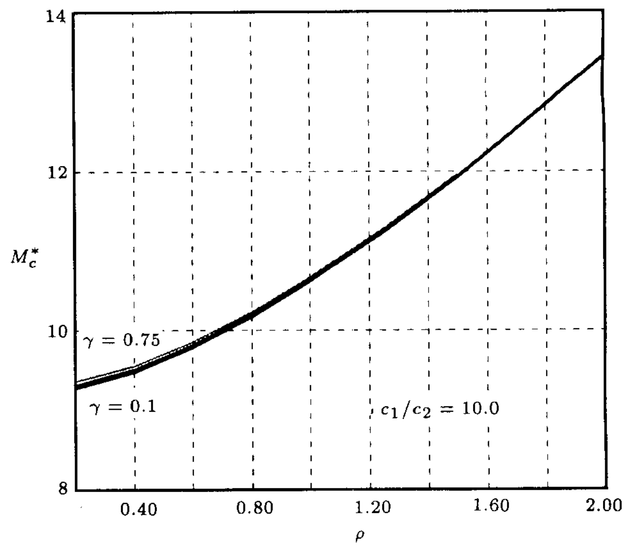

Figure 5g. Limit hoop moment versus ρ for $\alpha = 10.0$.

3. Figures 2 and 5, Equations 14 and 38 and Table 1 indicate that for all cases of loading, as limit moment increases, the value of Ω (plastic hinge length parameter) decreases. This means that for a fixed combination of γ and ρ, as attachment size parameter, α, increases, the region of plastic deformation becomes more localized to an area in

the vicinity of the attachment. It is also true that if α and γ are fixed the plastic zone decreases while ρ is increased. Comparison of the present results and [13] also indicates that for any given geometry, a radial load gives a greater plastic extent than that for moment loading;

4. Comparison between longitudinal and circumferential limit moments shows that for the same geometrical conditions, as ρ rises, the increase of circumferential loading moment is slightly less than the increase of longitudinal moment. This difference for high values of α becomes more significant;
5. For high values of α (i.e., 2, 4 and 10), increase of ρ has less effect on the increase of the limit load. This means that as α rises, the slope of the curve decreases. The reason is thought to be that when the circumferential dimension is small, a higher load is required in order that the surface is deformed plastically;
6. Table 1 gives the values of M_l^* for longitudinal bending moment and corresponding plastic extent parameters Ω_1 and Ω_2 when $\alpha = 1$. A reference to the solution of the system of Equation 26 indicates that for values of ρ up to $\rho = 1.8$, the improved solutions are close to those of [11]. With greater values of ρ there is significant divergence. The divergence of limit load for ρ greater than 1.8 could be attributed to the unrealistic attachment size or odd mechanism shape, resulted from such a value of ρ. In fact, for a fixed value of a and t and $\rho = 2, b$ is four times greater than plastic length in the axial direction, which is physically unacceptable;
7. Generally, using a 2-moment interaction yield surface needs some modifications in calculated limit load. For example, it can be shown that this yield condition reduced by a scale factor 0.618 is wholly within the true interaction surface for a shell made of material which follows the Tresca yield criterion [14]. Thus, the true load for Tresca yield condition is between 0.618 and 1 times the plastic collapse load calculated using the limited interaction surface. Therefore, the upper bounds calculated for this approximate yield surface are also upper bounds for a Tresca yield surface. More discussion concerning reduction factors required as a result of using 2-moment interaction yield condition can be found in [13,15,16];
8. It is expected to obtain a better approximation to the limit load if a more realistic yield condition is employed, though the analysis becomes more complex. Many researchers have employed the yield surface proposed by Illyushin, based on Von Mises criteria [16], to obtain an improved limit load. For example, Foo in [17] has used this yield surface to obtain the lower bound to the limit load and torque of cylindrical shells with a single cutout.

An extension of the present work is to employ the above mentioned yield surface. Also, a lower bound analysis of the present case would be informative for comparison purposes.

ACKNOWLEDGMENT

The author is indebted to Prof. R. Kitching for his invaluable advice and guidance given in the duration of this research program.

REFERENCES

1. Bijlaard, P.P. "Stresses from radial loads in cylindrical pressure vessels", *Welding J. Research Supplement*, **33**, pp 15-23 (1954).
2. Bijlaard, P.P. "Stresses from local loading in cylindrical pressure vessels", *Trans. ASME*, **77**, pp 805-816 (1955).
3. Bijlaard , P.P. "Stresses from radial loads and external moments in cylindrical pressure vessels", *Welding J. Research Supplement*, pp 23-608 (1955).
4. Bijlaard, P.P. "Additional data on stresses in cylindrical shells under local loading", *Welding Research Council Bulletin*, **50** (1959).
5. Witchman, K.R., Hopper, A.G. and Mershon, J.L. "Local stresses in spherical and cylindrical shells due to external loadings", *Welding Research Council Bulletin*, **107** (1980).
6. Findlay, G.E. and Timmins, W. "Local radial loads on cylinders: BS 5500 predictions versus experimental results", *Int. J. Pres. Ves. & Piping*, pp 33-48 (1987).
7. Tooth, A.S. and Motashar, F.A. "Radial loading of a cylindrical vessel through a rectangular rigid attachment", *Int. J. Pres. Ves. & Piping*, **37**, pp 345-63 (1989).
8. Symonds, P.S. "Limit analysis", In *Handbook of Engineering Mechanics*, W. Flugge, Ed., McGraw-Hill (1962).
9. Hodge, P.G., *Limit Analysis of Rotationally Symmetric Plates and Shells*, Prentice-Hall (1963).
10. Kitching, R., Hughes, J.F. and Jones, N. "Limit loading of cylindrical shells subjected to local circumferential bending moments", *Int. J. Mech. Sci.*, **20**, pp 61-81 (1978).
11. Kitching, R., Hussein, D. and Jones, N. "Limit loads for cylindrical shells subjected to local longitudinal bending moments", *Int. J. Mech. Sci.*, **24**, pp 673-90 (1982).

12. Rahimi, G.H. "Lower bound analysis of cylindrical shells subjected to local radial load", *Amir Kabir J.*, Amir Kabir University, Tehran (in Persian) (1988).
13. Rahimi, G.H. "Upper bound analysis of cylindrical shells subjected to local loads", *Scientia Iranica*, **4**(5) (1999).
14. Hodge, P.G. Jr "Yield conditions for rotationally symmetric shells under axi-symmetric loading", *J. Appl. Mech.*, pp 323-331 (1960).
15. Onat, E.T. and Prager, W. "Limit analysis of shells of revolution", *Proc. Roy. Netherland Acad. Sci.*, pp 534-548 (1954).
16. Robinson, M. "A comparison of yield surfaces for thin shells", *Int. J. Mech. Sci.*, **13**, pp 345-54 (1971).
17. Foo, S.S.B. "On the limit analysis of cylindrical shells with a single cutout", *Int. J. Pres. Ves. & Piping*, **49**, pp 1-16 (1992).